SMiRT–12 / K. Kussmaul (Editor)
1993 Elsevier Science Publishers B.V.

DYNAMIC COUPLING EFFECTS FOR TUNED STRUCTURAL SUBSYSTEMS

D.M. Ghiocel[1] and D. Ghiocel[2]

[1]Dept. of Civil Engineering, Case Western Reserve University, Cleveland, OH 44106, USA
[2]Civil Engineering Institute of Bucharest, Lacul Tei 124, Bucharest 72302, Romania

ABSTRACT

The paper investigates the effects of the seismic dynamic coupling between structural subsystems having tuned natural modes with sensibly different modal masses. The coupled subsystems are considered to have separate supports. A significant part of the vibration energy is transferred due to the dynamic coupling from one structural subsystem to another structural subsystem. The coupling effect is favorable for the heavy subsystem and unfavorable for the light subsystem, quite similar as for cascaded subsystems. Firstly, to illustrate the dynamic coupling effect the complex frequency approach is used to derive the transfer functions for two elastically fully coupled subsystems subjected to seismic base motions. Cascaded subsystems are defined as a particular case of the coupled subsystems for which the feedback effect from the light system is negligible. Secondly, the dynamic coupling effects are evaluated for two practical design situations via finite element seismic analyses: (i) Heavy Turbine Building with a U-shape in horizontal plane, i.e. the lateral wing substructures are coupled, and (ii) Reactor Building and Turbine Building, the two structure are coupled through the surrounding soil deposit. The implication of the dynamic interaction effects in NPP design may be significant as shown herein.

1 THEORETICAL BACKGROUND

Let consider the two degree of freedom system shown in the figure 1. The steady state response for this system subjected to seismic forces can be easily computed using the frequency response approach. The transfer function matrix of the system $\mathbf{H}(i\omega)$ is:

$$\mathbf{H}(i\omega) = \mathbf{Z}(i\omega)^{-1} = [-\omega^2\mathbf{M} + i\omega\mathbf{C} + \mathbf{K}]^{-1} \tag{1}$$

in which $\mathbf{Z}(i\omega)$ is the impedance matrix and **M**, **C** and **K** are the mass, damping and stiffness matrices of the system. The computation of the elements of the impedance matrix is straight forward from the system matrices:

$$\begin{aligned}
z_{11}(i\omega) &= -\omega^2 m_1 + i\omega(c_1 + c_2) + k_1 + k_2 \\
z_{12}(i\omega) &= z_{21}(i\omega) = -i\omega c_2 - k_2 \\
z_{22}(i\omega) &= -\omega^2 m_2 + i\omega(c_2 + c_3) + k_2 + k_3
\end{aligned} \tag{2}$$

Then, the elements of the transfer function matrix are derived:

$$h_{11}(i\omega)=\frac{z_{22}(i\omega)}{\mathrm{Det}(\mathbf{Z}(i\omega))}\ ,\ h_{12}(i\omega)=h_{21}(i\omega)=\frac{-z_{12}(i\omega)}{\mathrm{Det}(\mathbf{Z}(i\omega))}\ \text{and}\ h_{22}=\frac{z_{11}(i\omega)}{\mathrm{Det}(\mathbf{Z}(i\omega))} \tag{3}$$

where the determinant $\mathrm{Det}(\mathbf{Z}(i\omega))$ is: $\mathrm{Det}(\mathbf{Z}(i\omega))=z_{11}(i\omega)z_{22}(i\omega)-z_{12}(i\omega)^2$

Further, the system is excited at the two supports by a unit harmonic base motion. The amplitudes of the harmonic inertial forces of the system are $F_{01}=m_1\omega^2$ and $F_{02}=m_2\omega^2$, respectively. The total response is determined by the superposition of the load effects. Finally, the amplitudes of the total displacement transfer functions for the two degrees of freedom are:

$$\begin{aligned}|h_1(i\omega)|&=\frac{1}{|\mathrm{Det}(\mathbf{Z}(i\omega))|}\{[(-\omega^2m_2+\bar{k}_2)m_1\omega^2+k_2m_2\omega^2]^2+[\bar{c}_2m_1\omega^3+c_2m_2\omega^3]^2\}^{\frac{1}{2}}\\|h_2(i\omega)|&=\frac{1}{|\mathrm{Det}(\mathbf{Z}(i\omega))|}\{[(-\omega^2m_1+\bar{k}_1)m_2\omega^2+k_2m_1\omega^2]^2+[\bar{c}_1m_2\omega^3+c_2m_1\omega^3]^2\}^{\frac{1}{2}}\end{aligned} \tag{4}$$

where $|\mathrm{Det}(\mathbf{Z}(i\omega)|=\{[+m_1m_2\omega^4+\bar{k}_1\bar{k}_2-m_1\omega^2\bar{k}_2-m_2\omega^2\bar{k}_1-\omega^2\bar{c}_1\bar{c}_2-k_2^2+\omega^2c_2^2]^2$
$+[\omega\bar{c}_1(-m_2\omega+\bar{k}_2)+\omega\bar{c}_2(-m_1\omega+\bar{k}_1)-2\omega c_2k_2]^2\}^{1/2}$

The variables $\bar{k}_1=k_1+k_2, \bar{c}_1=c_1+c_2$ and $\bar{k}_2=k_2+k_3$, $\bar{c}_2=c_2+c_3$ are the effective stiffness and the effective damping corresponding to the first and the second degree of freedom, respectively. From the above expressions it has be observed that the two degree of freedom system can be represented by two coupled single degree of freedom oscillators having the stiffnesses and dampings equal to the effective ones defined above. The maximum dynamic coupling effects occur when the two coupled oscillators are tuned, i.e. the two frequencies $\omega_1=(\bar{k}_1/m_1)^{1/2}$ and $\omega_2=(\bar{k}_2/m_2)^{1/2}$ are equal. The figures 2,3,4 and 5 show some numerical evaluations of the analytical expressions for the case of tuned coupled oscillators. In the figure 2 the transfer functions computed for coupled oscillators and cascaded oscillators, i.e. no feedback effect as $k_3=0$ and $c_3=0$, are compared with that computed for uncoupled oscillators. The mass ratio m_1/m_2 is ten. For the second oscillator the peak spectral response is around two times larger for the fully coupled oscillators and three times larger for the cascaded oscillators than for the uncoupled oscillators. For the first oscillator the spectral peak is significantly reduced for the coupled and cascaded oscillators.

The effect of dynamic coupling is favorable for heavy subsystems and unfavorable for light subsystems. This result is well-known for cascaded subsystems, but less-known for fully coupled systems excited separately by seismic base motions. In the figure 3 are plotted the transfer functions for the tuned fully coupled oscillators having different values of the coupling stiffness k_2. It can be observed that for coupled oscillators the change in the coupling stiffness has a small effect on the amplitude of the spectral peaks, but has a large effect on the corresponding frequencies. The figure 4 shows that for a small coupling stiffness the dynamic interaction between the tuned oscillators is still large, but in this case the resonant frequency remains almost unchanged. This behavior is qualitatively different than that for cascaded oscillators with the same mass ratio. In the figure 5 is shown the transfer functions for larger

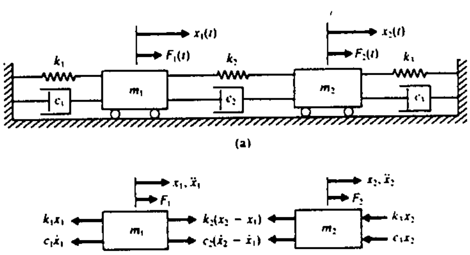

a) Horizontal coupling

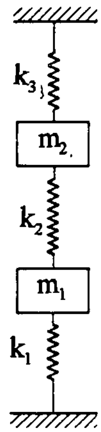

Figure 1 Two degree of freedom dynamic system.

b) Vertical coupling

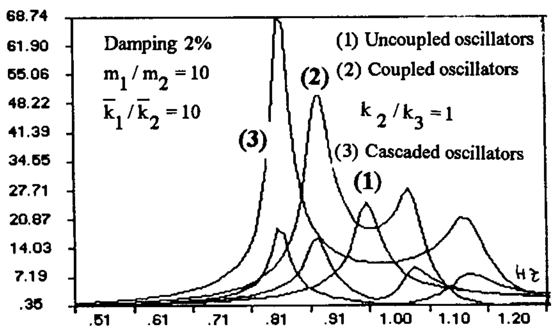

Figure 2. Transfer functions for uncoupled, cascaded and coupled oscillators.

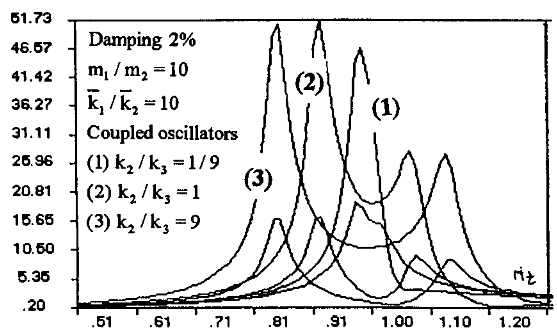

Figure 3. Transfer functions for coupled oscillators with different coupling stiffness

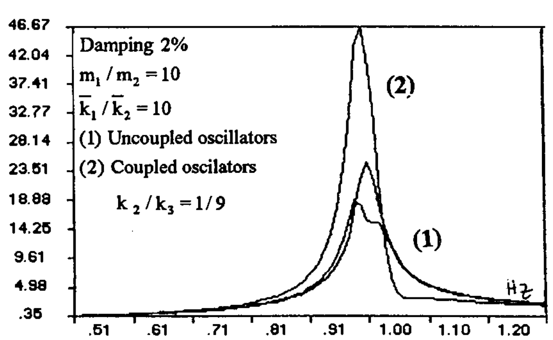

Figure 4. Transfer functions for uncoupled and weakly coupled oscillators.

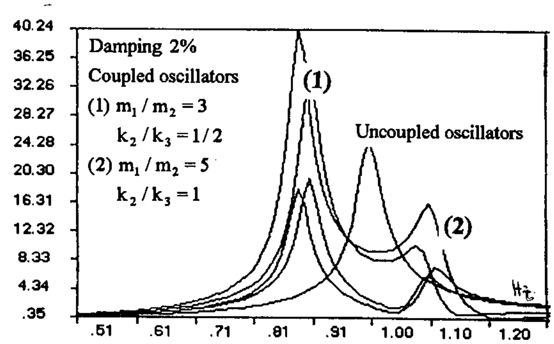

Figure 5. Transfer functions for coupled oscillators with low mass ratios.

mass ratios of the coupled oscillators. The effect of the dynamic coupling is considerable. Such situations are unfortunately often met in structural design of NPP.

2 CASE STUDIES

The dynamic coupling effects are evaluated for two practical structural designs via finite element seismic analyses: (i) Heavy Turbine Building with a U-shape in horizontal plane, the lateral wing substructures are coupled, and (ii) Reactor Building and Turbine Building, the two structure are coupled through the surrounding soil deposit.

The Turbine Building structure is shown in the figure 6. It is a composite structure with the lower part built in reinforced concrete and with the upper part built in steel. The structural deformed shape to seismic excitation shows that the response has quite different amplitudes for the two wing substructures. Substructure A is severely excited having a displacement considerably larger than that of substructure B. The figure 7 compares the largest FRS computed for the top level of the reinforced part for the two wing substructures.If the stiffness of the connection substructure C is removed the two wing substructures vibrates uncoupled. In this case the response of the substructures A+C and B+C is practically the same, the FRS having very close amplitudes and shapes. If the substructure C has non zero stiffness the two wing substructures behaves as coupled subsytems. The mass ratio is around four. The figure 7 can be favorably compared with the figure 5. In the figure 8 is plotted the FRS for the substructure at the roof level. The seismic response at this level is reduced as a result of the large in plane stiffness of the roof steel structure.

In the figure 9 is illustrated the structure-soil-structure model used to evaluate the dynamic coupling between the Reactor Building and Turbine Building through the surrounding soil. Obviously, the extension of the finite element mesh is much larger within soil deposit than shown in the figure. The seismic analysis is performed in two steps. The first step refers to the coupled seismic analysis using the overall model shown in the figure 9, while the second step refers to the uncoupled detailed analyses using refined models for the two buildings excited by the multiple base motions computed in the first step. In the figure 10 a is illustrated the spatial finite model used in the second step for the Internal Structure of the Reactor Building. Local amplification of vibrations are noticed at the top level where are the boxes of the steam generators, as shown in the figure 10 b. The FRS curves 1 and 2 in the figure 11 are computed at the bottom and at the top of the generator boxes when the structure-structure coupling through the soil deposit is neglected. The FRS curve 3 includes the effect of the coupling for soft soil conditions. The effect is large for the resonant spectral peak of the FRS curves. This behavior is the result of the coupling between two tuned modes of the two structures, more precisely of the horizontal interaction mode of the Turbine Building with the local vibration mode of the Internal Structure on the Reactor Building. The vibration energy is transferred from the mode with larger modal mass to the mode with mode with smaller modal mass.

It is shown herein that dynamic interaction effects for tuned fully coupled substructures may have a significant implication in design of NPP, as illustrated by the two case studies.

3 REFERENCES

Ghiocel, D.M., Mauna, T., Ghiocel, D.,(1991), the 2nd Int. Conf. on Recent Advances in Geotechnical Earthquake Engineering and Soil Dynamics,Vol.3, St. Louis, Missouri-Rolla.

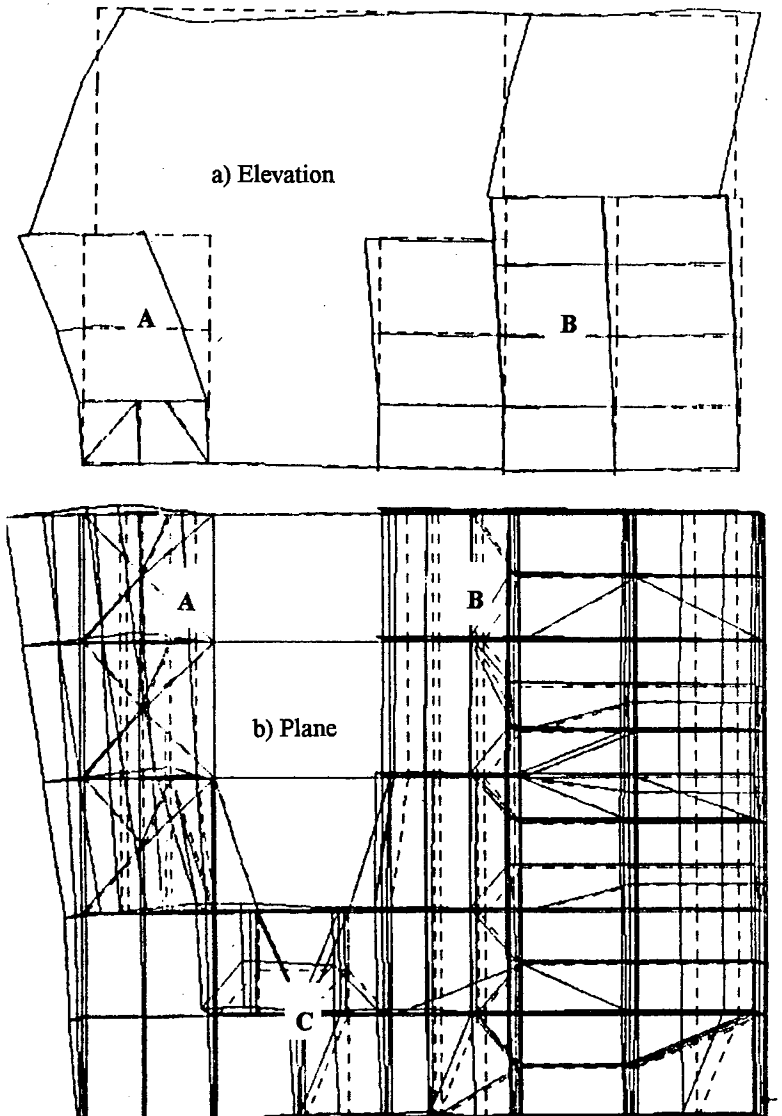

Figure 6. The Turbine Building structural model

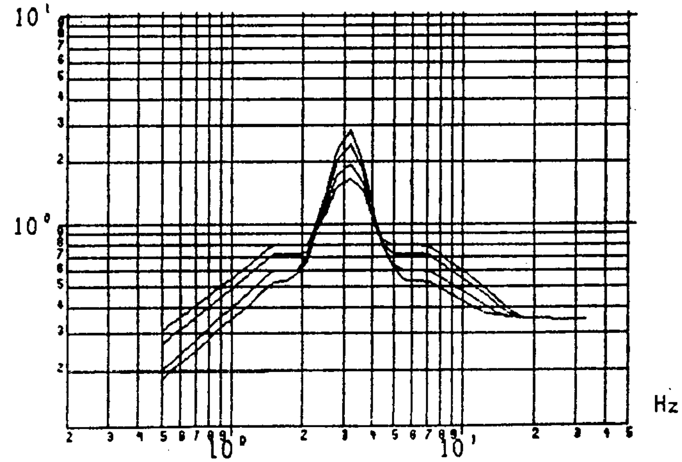

a) Substructure B

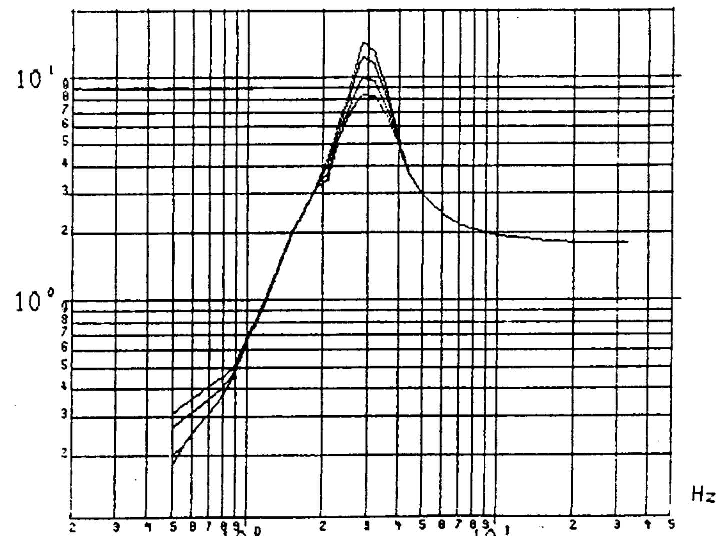

b) Substructure A

Figure 7 The FRS at the top level of the reinforced part

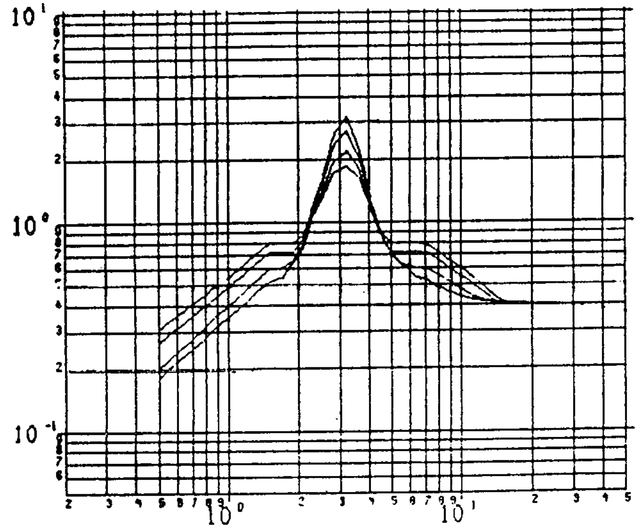

Figure 8. The FRS for the Substructure A at the roof level

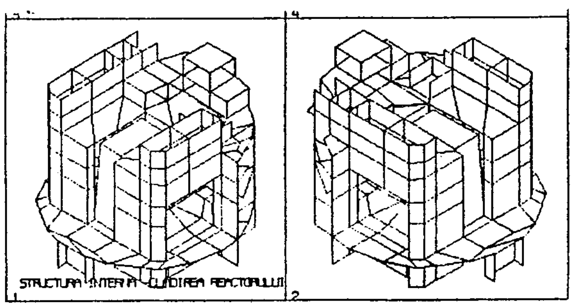

Figure 10 a). The Internal Structure model.

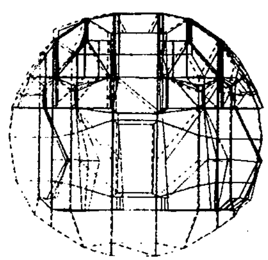

b) Local vibration mode

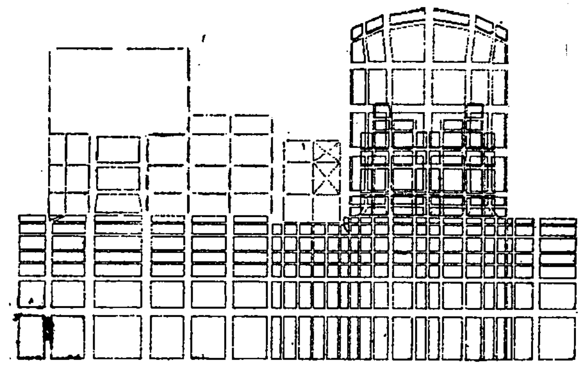

Figure 9. The structure-soil-structure model

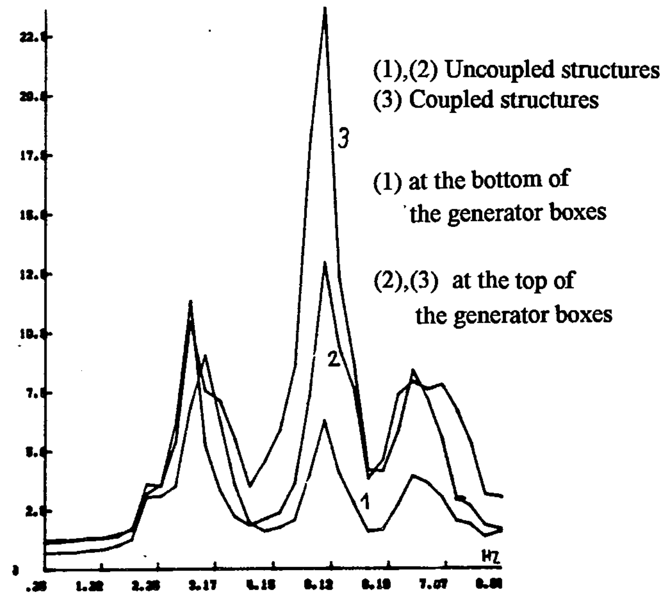

Figure 11. The FRS at the top of the Internal Structures;